Science Arts & Métiers (SAM)
is an open access repository that collects the work of Arts et Métiers Institute of Technology researchers and makes it freely available over the web where possible.

This is an author-deposited version published in: https://sam.ensam.eu
Handle ID: .http://hdl.handle.net/10985/12994

**To cite this version :**

Hussein ZAHR, Mohamed TRABELSI, Eric SEMAIL, Ngac Ky NGUYEN - Five-Phase Bi-Harmonic PMSM Control under Voltage and Currents Limits - In: IECON 2017 - 43rd Annual Conference of the IEEE Industrial Electronics Society ,, Chine, 2017-10 - Five-Phase Bi-Harmonic PMSM Control under Voltage and Currents Limits - 2017

Any correspondence concerning this service should be sent to the repository Administrator : scienceouverte@ensam.eu

# Five-Phase Bi-Harmonic PMSM Control under Voltage and Currents Limits

Hussein Zahr(1), Mohamed Trabelsi(1), Member IEEE, Eric Semail(1), Member IEEE, Ngac Ky Nguyen(1), Member IEEE

(1) Univ. Lille, Centrale Lille, Arts et Metiers ParisTech, HEI, EA 2697 - L2EP - Laboratoire d'Electrotechnique et d'Electronique de Puissance, F-59000 Lille, France
E-mails : (1){mohamed.trabelsi, hussein.zahr, eric.semail, ngacky.nguyen}@ensam.eu

***Abstract*— For a particular five-phase synchronous machine, this paper investigates the sensitivity of a vectorial control strategy on the required peak phase voltage whose value is fundamental for the choice of the DC bus voltage. The specificity of the machine is that the first and third harmonic components of the back electromotive force (back-emf) have the same amplitude. As a consequence, the torque can be produced by one of them or both with suitable currents. This degree of freedom is interesting for optimizing the efficiency and generating high transient torque. However, using two harmonics having the same amplitude leads to a necessity to analyze the constraints on the required phase machine voltage. Considering a Maximum Torque Per Ampere (MTPA) strategy, the paper examines the impact of some parameters such as the phase shift between currents and back-emfs or the ratio between the third and the first harmonic of current on the torque and maximum voltage value. Experimental tests with a limited DC bus voltage have been carried out and compared to the results obtained by a Finite Element Analysis.**

***Keywords*— *Bi-harmonic machine; control sensibility; Maximum Torque Per Ampere;***

## I. INTRODUCTION

Nowadays, multiphase machines are widely used for their fault tolerance and high torque density [1] especially in critical applications, such as marine [2], aerospace [3] and automotive traction [4]. Thanks to the vector control, these machines have an ability to produce torque without pulsation even with non-sinusoidal back-EMFs and non-sinusoidal currents, in similar way to the classical three-phase machines [5]. Moreover, in low voltage and/or high power applications, a high number of phases leads to a lower current per phase and consequently decreases the power of switches. Nevertheless, a high number of phases impact the cost since the number of drivers and current sensors increases, and the control is more complicated since many harmonics can interfere in torque production.

The work addressed in this paper deals with a five-phase PMSM that appears as a compromise when it used in critical applications such as automotive and aerospace applications. This machine allows creating torque from both 1st and 3rd harmonic components [6]. The contribution of each harmonic component depends mainly on the amplitude of the harmonic content of the back-EMF [7]-[8]. Generally, the 3rd harmonic is used to improve the torque, which comes essentially from the fundamental harmonic. Therefore, many researchers focus on modifying the control strategies, the design or both to achieve this goal. However, the torque production due to 3rd harmonic appears always to be marginal [9]-[12].

In this paper, the designed machine has a torque which can be created, with an equal sharing ratio between two harmonics since they have the same amplitude. This kind of machines is called bi-harmonic machine. Furthermore, in the machine design, many requirements for traction applications are considered:

1) High transient torque for a boost can be achieved by using the 3rd harmonic component.
2) Ability of control in wide speed range at constant power: for three-phase machine, the flux-weakening is appearing almost as the unique solution to increase the speed above the base speed when the maximum voltage imposed by the voltage source inverter is reached. For the bi-harmonic machine, many solutions exist for flux weakening operation since the 3rd harmonic offer an additional degree of freedom. The total torque/speed characteristic is the sum of the characteristic associated to each harmonic component [8][13].
3) Low losses associated to eddy currents when high frequency is required at high speed: the winding configuration is selected so that the harmonic content of the MMF is low. Consequently, low level of losses can appear in magnets. Therefore, the fractional slot concentrated winding with a number of slots per pole and per phase equal to 0.5 is used 0-[15].

The control strategies applied to multiphase machines are based on the Maximum Torque Per ampere MTPA [8]-0. Consequently, a ratio ρ between 1st and 3rd current harmonic components must be fixed to have collinear current and back-EMF (these assertions are detailed in section III). Practically, it could be appeared that the actual current differs from the optimal (reference) ones, leading to a variation (increase or decrease) of torque and required voltage.

The aim of this paper is to study the sensitivity of the MTPA strategy. Taking into account the several degrees of freedom in the case of the 5-phase bi-harmonic PMSM (5-Φ B-PMSM), there are several possibilities to modify the

reference currents by acting on the phase shift (φ) between current and back-EMF and/or the ratio between the 1st and 3rd harmonic current components (ρ). Consequently, in addition to the classical MTPA method, two new strategies will be investigated and analyzed with constraints on the voltage and currents.

This paper will be organized as follows: Section II presents the structure of the considered prototype. Section III presents the MTPA supply strategies applied to the 5-Φ B-PMSM machine and the other strategies derived from the MTPA but with the variation of the phase shift φ and the ratio $\rho=I_3/I_1$. The obtained characteristics of the studied machine under these conditions are analyzed, taking into account the voltage and current limits.

## II. Topology and Vector Control of Invistigated 5-Φ Bi-harmonic PMSM

This section aims to present the prototype of the five phase bi-harmonic PMSM and the adopted control for operating characteristics investigation. The investigated machine can be used in traction applications with capability for developing high torque during transient operation and good efficiency at steady state [16]-[17].

### *A. 5-Φ Bi-Harmonic PMSM Topology*

The prototype is depicted in Fig.1. This prototype consists in a 5-Φ 40-slot/16-pole bi-harmonic PMSM [8]0. In order to decrease the cogging torque and other torque ripples, the stator is skewed by ½ slot step. In the next section, thanks to vector control, the ability to produce torques with low torque ripples even when two harmonics are injected is verified and approved.

The back-EMF harmonic content, obtained for a 500 rpm rotor speed, is depicted in **Erreur ! Source du renvoi introuvable.**Fig. 3. It comprises two main harmonic components ($E_1$ and $E_3$). Here, it should be noticed that because of a high value of winding factor, the 3rd harmonic component of the back-EMF is greater than the fundamental harmonic, but both have comparable magnitude since they have a ratio $\rho = E_3/E_1=1.22$. It should be noticed also that, for a 5-Φ 40-slot/16-pole, this ratio-value allows to maximize the torque in low-speed region and to improve the flux-weakening operation mode [7][8]0.

### *B. Modeling of the 5-Φ Bi-harmonic PMSM*

In this part, the basic knowledge of the reference frame theory applied to a 5-Φ B-PMSM is introduced to highlight the potentialities of this concept used for vector control of multiphase machines. The basics of the vector control for multiphase machines [18]-[19], leads to three decoupled sub-spaces, as shown in Fig. 4.

- First sub-space: is associated mainly with the 1st harmonic electrical components (voltage, current, back-EMF) corresponding to the Main fictitious Machine (MM) and is noted with index (αβ).
- Second sub-space: is associated with the 3rd harmonic component corresponding to the Secondary fictitious Machine (SM) and is noted with index (xy).
- Third subspace: is associated with the fifth harmonic component. Because of the star connection isolated neutral of the PMSM, there is no path for the zero-sequence component of current.

(a) Stator (b) Rotor

Fig. 1. Machine prototype (5-Φ 40-slot/16-pole/48-pole).

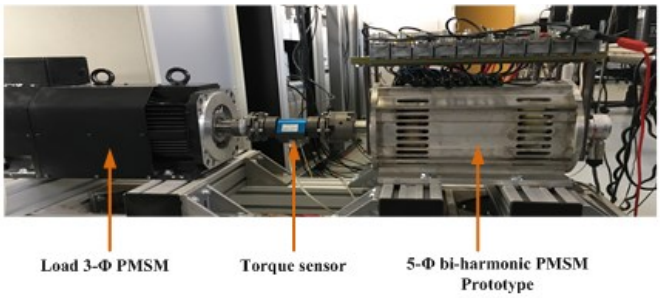


Fig. 2. Test bench used for experimental validation.

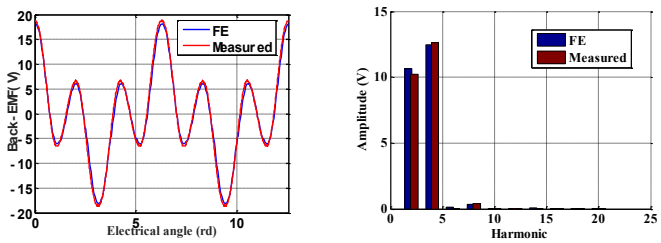


(c) (d)

Fig. 3. Waveforms and harmonic content of the back-EMF obtained by FE and experimentally at XX rpm

The transformation which allows to obtain these machines is the generalized Concordia transform. The equivalent components in orthogonal sub-spaces αβ and xy are obtained by:

$$\left[x_{\alpha\beta}\right]=\sqrt{\frac{2}{5}}\left[C_{\alpha\beta}\right]\left[x_n\right] \quad (1)$$

$$\left[x_{xy}\right]=\sqrt{\frac{2}{5}}\left[C_{xy}\right]\left[x_n\right] \quad (2)$$

where :

$$\left[C_{\alpha\beta}\right]=\begin{bmatrix}1 & \cos\frac{2\pi}{5} & \cos\frac{4\pi}{5} & \cos\frac{6\pi}{5} & \cos\frac{8\pi}{5}\\ 0 & \sin\frac{2\pi}{5} & \sin\frac{4\pi}{5} & \sin\frac{6\pi}{5} & \sin\frac{8\pi}{5}\end{bmatrix} \quad (3)$$

$$\left[C_{xy}\right]=\begin{bmatrix}1 & \cos\frac{4\pi}{5} & \cos\frac{8\pi}{5} & \cos\frac{12\pi}{5} & \cos\frac{16\pi}{5}\\ 0 & \sin\frac{4\pi}{5} & \sin\frac{8\pi}{5} & \sin\frac{12\pi}{5} & \sin\frac{16\pi}{5}\end{bmatrix} \quad (4)$$

$$\left[X_{d1q1}\right]=\underbrace{\begin{bmatrix}\cos\theta_m & \sin\theta_m\\ -\sin\theta_m & \cos\theta_m\end{bmatrix}}_{\substack{\textit{Park transformation}\\ \textit{applied to MM}}}\left[x_{\alpha\beta}\right] \quad (5)$$

$$\left[X_{d3q3}\right]=\underbrace{\begin{bmatrix}\cos 3\theta_m & -\sin 3\theta_m\\ \sin 3\theta_m & \cos 3\theta_m\end{bmatrix}}_{\substack{\textit{Park transformation}\\ \textit{applied to SM}}}\left[x_{xy}\right] \quad (6)$$

$[x_n]$ denotes the variable in natural frame *abcde* (voltage, current, back-EMF, ...). Their equivalent components in orthogonal frames are denoted by $[x_{\alpha\beta}]$ and $[x_{xy}]$. $[x_{d1q1}]$ and $[x_{d3q3}]$ are variables in rotating frame.

For an easier control of the 5-Φ B-PMSM, the Park transformation given in (5)-(6) is used. In such frames, the currents, the voltages and the flux are constant in healthy operations. Consequently, the control of the two-phase fictitious machines can be achieved independently with two PI-controllers. For motor modeling, we suppose that the magnetic saturation, the hysteresis and slot effects, and the iron losses are neglected. Considering these assumptions, the electrical equations that describe the 5-Φ Bi-harmonic PMSM, in dq-rotating frames, are defined by:

— for the fictitious main machine (MM)

$$\begin{cases} V_{d1} = RI_{d1} + L_{d1}\dfrac{dI_{d1}}{dt} + e_{d1} - \omega L_{q1}I_{q1} \\ V_{q1} = RI_{q1} + L_{q1}\dfrac{dI_{q1}}{dt} + e_{q1} + \omega L_{d1}I_{d1} \end{cases} \quad (7)$$

— for the fictitious Secondary machine (SM)

$$\begin{cases} V_{d3} = RI_{d3} + L_{d3}\dfrac{dI_{d3}}{dt} + e_{d3} + 3\omega_m L_{q3}I_{q3} \\ V_{q3} = RI_{q3} + L_{q3}\dfrac{dI_{q3}}{dt} + e_{q3} - 3\omega_m L_{d3}I_{d3} \end{cases} \quad (8)$$

where, ($[v_{dq1}]$, $[i_{dq1}]$, $[e_{dq1}]$) and ($[v_{dq3}]$, $[i_{dq3}]$, $[e_{dq3}]$) are the stator voltages, the phase currents and the back-EMFs linked to the fictitious MM and the fictitious SM, respectively. R is the phase resistance and ($L_{d1}$, $L_{q1}$) and ($L_{d3}$, $L_{q3}$) are the equivalent self-inductances linked to the MM and SM, respectively. The electrical fundamental pulsation corresponding to the MM, in steady state, $\omega_m$, is given by (9), where p is the pair poles number, fs is the electrical supply frequency and $\theta_m$ is the mechanical rotor position. On the

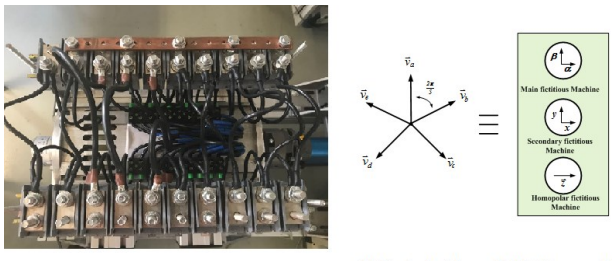


(a) Five phase PMSM in original frame

(b) Equivalent decoupled fictitious machines in decoupled sub-spaces

Fig.4. Configuration of the 5-Φ PMSM

TABLE I
ELECTRICAL PARAMETERS OF 5-**Φ B-PMSM**

| |
|---|
| *Rs* = 0.0324 Ω; *Lp* =139 *μH*; *Ls* = 178 *μH*, *p=8*, |
| *From spectrum analysis at no load for 500 rpm, amplitudes (RMS) of emf* $E_1$*=10,2V,* $E_3$*=13V* |

contrary, the electrical pulsation, $\omega_s$, corresponding to the SM, in steady state, is three times higher than $\omega_m$, as given by (10):

$$\omega_m = p\frac{d\theta_m}{dt} = p\Omega = 2\pi f_s \quad (9)$$

$$\omega_s = -3p\frac{d\theta_m}{dt} = -3p\Omega = -6\pi f_s \quad (10)$$

For the considered machine, the developed torque by the five-phase PMSM is the sum of the torque produced by each fictitious machine, which is given by:

$$T_{em} = \frac{5}{2.\Omega}(\underbrace{E_1 I_1 \cos(\varphi_1)}_{T_m} + \underbrace{E_3 I_3 \cos(\varphi_3)}_{T_s}) \quad (11)$$

where ($E_1$, $E_3$) and ($I_1$, $I_3$) are the 1st and the 3rd harmonic amplitude of the back-emf and current respectively, $\varphi_1(\varphi_3)$ the phase shift between the 1st (3rd) harmonic current and the 1st (3rd) harmonic of the back-emf.

## III. OPERATING CHARACTERISTICS OF 5-Φ BI-HARMONIC PMSM UNDER VOLTAGE AND CURRENT LIMITS

In this section, several supply strategies will be presented and examined in order to test the sensitivity of MTPA strategy applied to the 5-Φ Bi-Harmonic PMSM.

### *A. Maximum Torque Per Ampere strategy (MTPA).*

For this control strategy, the maximum torque is achieved when the back-emf and the current vectors are collinear [19]. The two following conditions guarantee the collinearity:

1) Based on equation (11), the maximum torque is guaranteed by setting :

$$\varphi_1 = \varphi_3 = 0 \quad (12)$$

2) The ratio between the 1st and the 3rd harmonic current component must be equal to ρ given by :

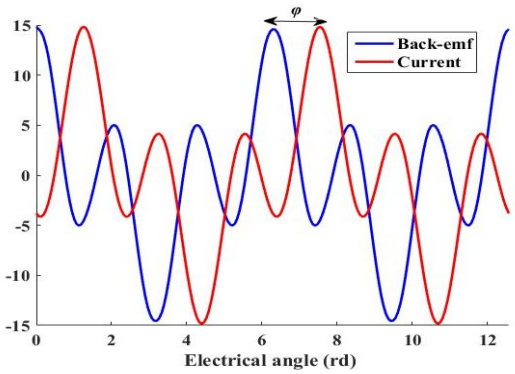


Fig. 5. Currrent and back-emf shape for φ≠0.

$$\rho = \frac{I_3}{I_1} = \frac{E_3}{E_1} \tag{13}$$

According to Fig. 3, the ratio ρ must be equal to 1.22. Assuming that the machine is supplied with currents characterized by equation (14):

$$\begin{cases} I_1 = \sqrt{2}\dfrac{1}{\sqrt{\rho^2+1}} I_{eff} \\ I_3 = \sqrt{2}\dfrac{\rho}{\sqrt{\rho^2+1}} I_{eff} \end{cases} \tag{14}$$

This strategy can be used as long as the maximum voltage delivered by the voltage source inverter (VSI) is not reached. When the maximum voltage is reached, the speed can still be increased by varying the ratio ρ and/or the phase shifts $\varphi_1$ and $\varphi_3$. This approach is different from the one used in classical three phase machines, in which flux-weakening appears as the only possible solution to increase speed when the voltage limit is reached. For the bi-harmonic machine, the determination of the current references in high speed zone requires the resolution of four variables non-linear optimization problem [8].

As mentioned in the introduction, the two strategies will be considered and compared with the MTPA:

- The first strategy: the phase shift $\varphi_1$ and $\varphi_3$ are fixed to zero, and the ratio ρ is variable.
- The second strategy: The ratio ρ is fixed to its optimal value and the phase shifts $\varphi_1$ and $\varphi_3$ are varying.

For each control strategy, the required voltage is calculated and compared with the one obtained in the MTPA strategy. The results are mainly presented from Fig. 7 to Fig. 10.

### *B. Control with ρ and variable phase shifts φ.*

In this control strategy, the value ρ is always equal to 1.22. However, the phase shifts $\varphi_1$ and $\varphi_3$ are changed so that the shape of the current remains the same as the one obtained with MTPA strategy. Therefore, we introduce a global phase shift between the current and the back-emf, noted φ as presented in Fig. 5. Consequently, the phase shift $\varphi_1$ and $\varphi_3$ are expressed in function of φ as follows:

TABLE II
INTERVAL OF VARIATION OF THE TORQUE AND PEAK VOLTAGE FOR EACH STUDIED CASE.

| | **Torque percentage variation** | **Voltage peak value percentage variation** |
|---|---|---|
| J=2.5A/mm$^2$ | $-28.3\% \le \Delta T \le 1\%$ | $-23.75\% \le \Delta V \le 12.46\%$ |
| J=5A/mm$^2$ | $-31.7\% \le \Delta T \le 0.86\%$ | $-39.9\% \le \Delta V \le 18.57\%$ |
| $I_{peak}$=200A | $-33.06\% \le \Delta T \le 0.25\%$ | $-40.1\% \le \Delta V \le 19.4\%$ |
| J=20A/mm$^2$ | $-35.49\% \le \Delta T \le 1.5\%$ | $-14.1\% \le \Delta V \le 8.4\%$ |

$$\begin{cases} \varphi_1 = \varphi \\ \varphi_3 = 3\varphi \end{cases} \tag{15}$$

The allowed variation of the phase shift φ belongs to the following interval:-π/10 ≤ φ ≤ π/10. The FE simulation is performed for a current density of 2.5 A/mm$^2$, 5A/mm$^2$ and 20A/mm$^2$. Another operating point is considered when the current peak value is equal to 200A. Here, it should be noticed that the maximum value which can be measured by the current sensors reaches 200A.

Each current density is injected in the machine for different speed value so that for φ=0, a peak voltage value equal to the half of DC bus voltage is obtained, for all the considered current densities. In this work, the DC bus voltage is assumed to be 48V. Fig. 6 and Fig. 7 present the variation of torque and voltage respectively according to the variation of phase shift φ. The results are determined using the FE software ANSYS Maxwell 2D. As observed in Fig. 6, the required voltage is greater than 24V when the phase shift φ<0.

Regarding Table. II, it has been shown that the percentage of the additional required voltage is within the band [8%-20%].

On the contrary, the required voltage becomes less than 24 V when φ>0. The percentage of required voltage decrease is within [14%-40%] in comparison to the MTPA value (24V).

In Fig. 8, the impact of phase shift on the voltage waveform is presented. The FE simulation is performed for three of phase shift values (φ=-π/10, φ=0 and φ=π/10) with a current density equal to 20A/mm$^2$. The results show that for φ=-π/10, the voltage exceeds for several instants the maximum limit of 24V. Consequently, an important distortion can appear in the voltage waveform in this case.

In addition, the torque can decrease significantly by 35.9% as depicted in table .II and Fig. 6 when the phase shift φ<0 or φ>0.07. In order to compensate this torque decrease, more current density must be injected which increases significantly the required voltage. Notice that, in all the studied cases, a slight improvement of the torque is possible when φ is within [0-0.07] (up to 1.5 % according to Table. II and to Fig. 4), due to the slight saliency effect of the machine.

### *C. Control with variable value of ρ and phase shift φ equal to zero.*

In this control strategy, the phase shift $\varphi_1$ and $\varphi_3$ are fixed to zero. The ratio between the 1$^{st}$ and the 3rd harmonic current ρ is variable. This means that the error on the ratio ρ (<1.22) implies that the torque is mainly produced by the 1$^{st}$ harmonic

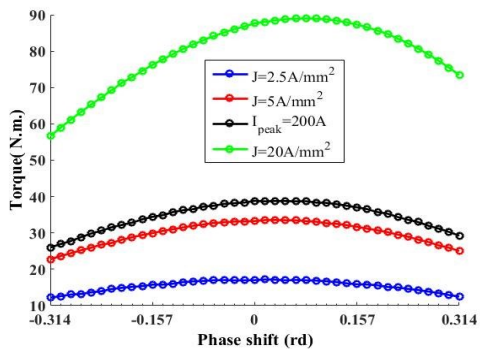


Fig. 6. Variation of torque according to the phase shift angle φ.

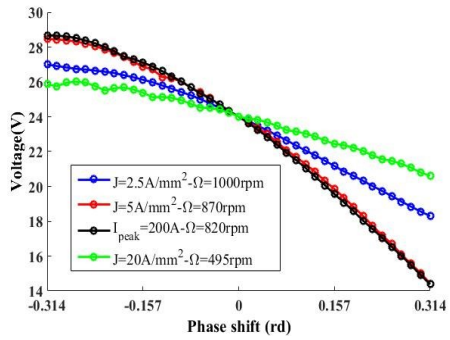


Fig. 7. Variation of torque according to the phase shift angle φ.

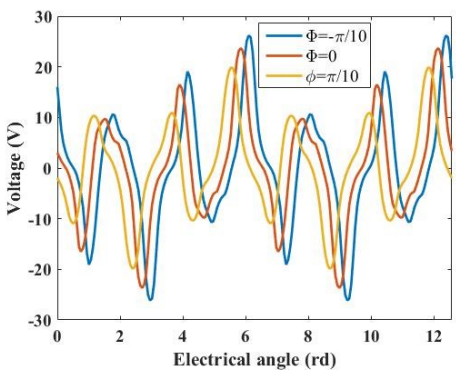


Fig. 8. Voltage waveform for three value of phase shift φ and a current density of 20A/mm$^2$ obtained by FE simulation.

component. In addition, the machine should deliver the same torque as the one delivered when the MTPA strategy is applied. In these conditions, the toque is given by:

$$T_{em} = \frac{5}{2\Omega}(E_1 I_1 + \rho E_3 I_1) = T_{MTPA} \qquad (16)$$

In MTPA conditions, the ratio $\rho_{MTPA}$=1.22, this results in:

$$I_1(\rho) = \frac{\Omega T_{MTPA}}{5/2(E_1+\rho E_3)} = \frac{\sqrt{2}\dfrac{I_{eff}}{\sqrt{\rho_{MTPA}^{\ 2}+1}}(E_1+\rho_{MTPA}E_3)}{(E_1+\rho E_3)} \qquad (17)$$

In Fig. 9, we present the ratio between the current density due to the variation of the ratio ρ and the current density of the MTPA strategy $J/J_{MTPA}$. Results show that it is necessary to inject more current density in the machine in order to

TABLE III
ADVANTAGES AND DRAWBACKS OF THE TWO STUDIED STRATEGIES

| | **Variation of φ** (ρ=1.22) | **Variation of ρ** (φ=0) |
|---|---|---|
| Advantages | 1-Less required voltage than MTPA strategy if φ>0<br>2-Same current peak value as MTPA | 1-Less required voltage than MTPA for the same torque |
| Drawbacks | 1-More required voltage than the MPTA strategy if φ<0<br>2-Generally, lower torque than the once in MTPA is obtained. | 1-More copper losses than MTPA are obtained for the same torque.<br>2-Higher peak current than MTPA strategy |

maintain the same torque as the MTPA approach. This results in more copper losses in the 5-Φ Bi-Harmonic PMSM machine. The variation of the required voltage value according to ρ is given in Fig. 10. These values are measured experimentally and compared to the ones obtained by FE simulation. We can conclude that they are quite similar.

We show that when the variation of the ratio ρ is less 1.22 (MTPA ratio), the required voltage is generally lower. If ρ=0- which means that there is no 3$^{rd}$ harmonic current component- the required voltage is 3% less than the MTPA case at 963rpm, 11% at 790 rpm and 12% at 640rpm. The lower is the contribution of the 3$^{rd}$ harmonic in the total torque; the lower is the required voltage. This is due mainly to the fact that the 3$^{rd}$ harmonic induces more voltage drop than the 1$^{st}$ harmonic. Fig. 11 shows a comparison between the phase voltage obtained by FE simulation and the measured voltage obtained after elimination of PWM harmonics. Finally, by comparing the two approaches developed in section III.B. and III. C., it appears that the required voltage is less sensitive to the variation of ρ than the variation of φ. Finally, Table.III summarizes the advantages and drawbacks of each control strategy in terms of peak current, peak voltage, torque and copper losses.

## IV. CONCLUSION

In this paper, the sensitivity of MTPA strategy was investigated for a particular bi-harmonic machine whose the torque developed from the 1$^{st}$ harmonic is equivalent to the one from the 3$^{rd}$ harmonic. Given that the MTPA is achieved when $\rho_{MTPA}=I_3/I_1=E_3/E_1$ and φ=0, two sensitivity tests are performed: the first one concerns the phase shift φ (control parameter) between the current and the back-emf. The second one concerns the ratio $\rho=I_3/I_1$(design parameter) which is equal in MTPA to $E_3/E_1$. The results show that if the phase shift φ varies between -π/10 and π/10, the torque is thus reduced up to 35%. Therefore, in order to obtain the desired torque, more current density should be injected in the machine. Furthermore, the required voltage can increase up to 20% (φ<0) or decreases by 40% (φ >0) compared to MTPA values.

On the other hand, the variation on the ratio ρ can decrease slightly the required voltage between 3% and 12%, while keeping the same torque as the one provided in MTPA

strategy. But for this kind of variation, the current density must be increased.

In conclusion, the sensitivity of the required voltage and current with respect to ρ and φ should be taken into account when sizing the VSI. The presented results allow to define the security margin to be considered when fixing the volt-ampere rating of the VSI. Consequently, the machine remains able to provide the same torque as the one delivered in MTPA when the values of ρ and φ are not precisely determined.

## ACKNOWLEDGEMENT

This work has been achieved within the framework of CE2I project (Convertisseur d'Energie Intégré Intelligent). CE2I is co-financed by European Union with the financial support of European Regional Development Fund (ERDF), French State and the French Region of Hauts-de-France.

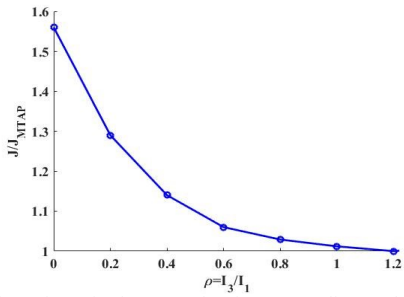


Fig. 9. Variation of required current density J according to the ratio $\rho$.

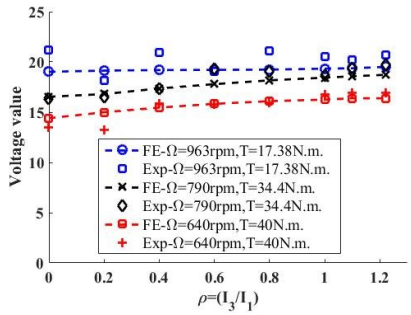


Fig. 10. Variation of required voltage according to the ratio $\rho$.

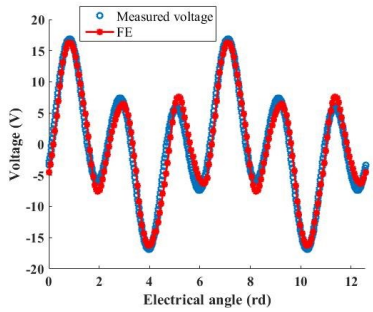


Fig. 11. Voltage waveform for ρ=1.1 and N=640rpm

## REFERENCES

[1] F. Barrero and M. J. Duran, "Recent advances in the design, modeling and control of multiphase machines—Part 1," *IEEE Trans. Ind. Electron.*, vol. 63, no. 3, pp. 449-458, Jan. 2016.

[2] J. S. Thongam, M. Tarbouchi, A. F. Okou, D. Bouchard and R. Beguenane, "Trends in naval ship propulsion drive motor technology," *2013 IEEE Electrical Power & Energy Conference*, Halifax, NS, 2013, pp. 1-5.

[3] R. Bojoi, A. Cavagnino, A. Tenconi and S. Vaschetto, "Control of Shaft-Line-Embedded Multiphase Starter/Generator for Aero-Engine," in *IEEE Transactions on Industrial Electronics*, vol. 63, no. 1, pp. 641-652, Jan. 2016.

[4] L. Parsa and H. A. Toliyat, "Fault-Tolerant Interior-Permanent-Magnet Machines for Hybrid Electric Vehicle Applications," in *IEEE Transactions on Vehicular Technology*, vol. 56, no. 4, pp. 1546-1552, July 2007.

[5] J. Wang, L. Zhou and R. Qu, "Harmonic current effect on torque density of a multiphase permanent magnet machine," *2011 International Conference on Electrical Machines and Systems*, Beijing, 2011, pp. 1-6.

[6] F. Scuiller, E. Semail and J.F. Charpentier, "Multi-criteria based design approach of multiphase permanent magnet low-speed synchronous machines," *IET Electr. Power appl,,* 2009, vol.3, Iss.2, pp.102-110.

[7] B. Aslan and E. Semail, "New 5-phase concentrated winding machine with bi-harmonic rotor for automotive application," *2014 International Conference on Electrical Machines (ICEM)*, Berlin, 2014, pp. 2114-2119.

[8] H. Zahr, J. Gong, E. Semail and F. Scuiller, "Comparison of Optimized Control Strategies of a High-Speed Traction Machine with Five Phases and Bi-harmonic Electromotive Force," *Energies* 2016, Vol. 9, No. 12, pp. 1-19.

[9] M. Mengoni, L. Zarri, A. Tani, L. Parsa, G. Serra and D. Casadei, "High-Torque-Density Control of Multiphase Induction Motor Drives Operating Over a Wide Speed Range," in *IEEE Transactions on Industrial Electronics*, vol. 62, no. 2, pp. 814-825, Feb. 2015.

[10] A. Abdelkhalik, M. Masoud and W. Barry, "Eleven-phase induction machine: steady-state analysis and performance evaluation with harmonic injection," *in IET Electric Power Applications*, vol. 4, no. 8, pp. 670-685, Sept. 2010.

[11] Zhao, Pinzhi, and Guijie Yang. "Torque density improvement of five-phase PMSM drive for electric vehicles applications." *Journal of Power Electronics* 11.4 (2011): 401-407.

[12] K. Wang, Z. Q. Zhu and G. Ombach, "Torque Improvement of Five-Phase Surface-Mounted Permanent Magnet Machine Using Third-Order Harmonic," in *IEEE Transactions on Energy Conversion*, vol. 29, no. 3, pp. 735-747, Sept. 2014.

[13] H. Zahr, E. Semail, B. Aslan and F. Scuiller, "Maximum Torque Per Ampere strategy for a biharmonic five-phase synchronous machine," *2016 International Symposium on Power Electronics, Electrical Drives, Automation and Motion (SPEEDAM)*, Anacapri, 2016, pp. 91-97.

[14] B. Aslan, E. Semail and J. Legranger, "General Analytical Model of Magnet Average Eddy-Current Volume Losses for Comparison of Multiphase PM Machines With Concentrated Winding," in *IEEE Transactions on Energy Conversion*, vol. 29, no. 1, pp. 72-83, March 2014.

[15] N. Bianchi and E. Fornasiero, "Index of rotor losses in three-phase fractional-slot permanent magnet machines," in *IET Electric Power Applications*, vol. 3, no. 5, pp. 381-388, September 2009.

[16] I. Boldea, L. N. Tutelea, L. Parsa and D. Dorrell, "Automotive Electric Propulsion Systems With Reduced or No Permanent Magnets: An Overview," in *IEEE Transactions on Industrial Electronics*, vol. 61, no. 10, pp. 5696-5711, Oct. 2014.

[17] A.M. El-Refaie, "Motors/generators for traction/propulsion applications: A review," in *IEEE Vehicular Technology Magazine*, vol. 8, no. 1, pp. 90-99, March 2013.

[18] X. Kestelyn, E. Semail , "Vectorial modeling and control of multiphase machines with non-salient poles supplied by an inverter ",*Chap.5 in book " Control of non-conventional synchronous motors"*, ISTE Ltd and John Wiley & Sons Inc, 2012, 44 pages.

[19] X. Kestelyn and E. Semail, "A Vectorial Approach for Generation of Optimal Current References for Multiphase Permanent-Magnet Synchronous Machines in Real Time," in *IEEE Transactions on Industrial Electronics*, vol. 58, no. 11, pp. 5057-5065, Nov. 2011.